



UNIVERSIDADE ESTADUAL DE CAMPINAS  
SISTEMA DE BIBLIOTECAS DA UNICAMP  
REPOSITÓRIO DA PRODUÇÃO CIENTÍFICA E INTELLECTUAL DA UNICAMP

**Versão do arquivo anexado / Version of attached file:**

Versão do Editor / Published Version

**Mais informações no site da editora / Further information on publisher's website:**

<https://www.sciencedirect.com/science/article/pii/S0896844623001687>

**DOI: 10.1016/j.supflu.2023.106004**

**Direitos autorais / Publisher's copyright statement:**

©2023 by Elsevier. All rights reserved.

DIRETORIA DE TRATAMENTO DA INFORMAÇÃO

Cidade Universitária Zeferino Vaz Barão Geraldo

CEP 13083-970 – Campinas SP

Fone: (19) 3521-6493

<http://www.repositorio.unicamp.br>



# Removal of 5-hydroxymethylfurfural from brewer's spent grains hydrolysates obtained by subcritical water hydrolysis: An approach using liquid-liquid extraction

Tiago Linares Cruz Tabosa Barroso<sup>a,1</sup>, William Gustavo Sganzerla<sup>a,\*</sup>,  
Luiz Eduardo Nochi Castro<sup>a</sup>, Nicolás Luís Moreira Freiria<sup>b</sup>, Gerardo Fernández Barbero<sup>b</sup>,  
Miguel Palma Lovillo<sup>b</sup>, Maurício Ariel Rostagno<sup>c</sup>, Tânia Forster-Carneiro<sup>a,\*</sup>

<sup>a</sup> University of Campinas (UNICAMP), School of Food Engineering (FEA), Campinas, SP, Brazil

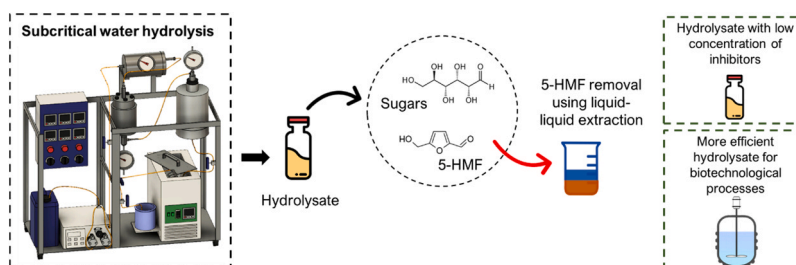
<sup>b</sup> Department of Analytical Chemistry, Faculty of Sciences, Agrifood Campus of International Excellence (ceiA3), IVAGRO, University of Cadiz, 11510 Puerto Real, Spain

<sup>c</sup> School of Applied Sciences (FCA), University of Campinas (UNICAMP), Limeira, SP, Brazil

## HIGHLIGHTS

- Subcritical water hydrolysis followed by liquid-liquid extraction of 5-HMF.
- Acetyl acetate effectively removed 5-HMF from BSG hydrolysate.
- Liquid-liquid extraction with acetyl acetate is an alternative for 5-HMF removal.
- The optimal conditions were pH 6.5, 35 °C, and volumetric ratio of 1:2 v/v.
- The maximum 5-HMF removal efficiency reached was 73.85 %.

## GRAPHICAL ABSTRACT



## ARTICLE INFO

### Keywords:

Lignocellulosic biomass  
Detoxification  
Fermentable sugars  
Hydrolysis  
Waste valorization  
Brewery residue

## ABSTRACT

This study evaluated the use of a semi-continuous subcritical water hydrolysis (SWH) process followed by liquid-liquid extraction to produce a concentrated hydrolysate with a low content of 5-hydroxymethylfurfural (5-HMF). The SWH was operated at 15 MPa, 180 °C, 5 mL min<sup>-1</sup>, and a solvent-to-feed ratio of 22.5 g g<sup>-1</sup>. The hydrolysate was subjected to liquid-liquid extraction at different pH (2.5–6.5), temperatures (25–45 °C), and volumetric ratios between hydrolysate and ethyl acetate (1:2–2:1 v/v) using the Box–Behnen design followed by response surface methodology. The optimal conditions for removing 5-HMF (73.85 %) were pH 6.5, 35 °C, and a volumetric ratio between hydrolysate and ethyl acetate of 1:2 (v/v). The hydrolysate presented a final composition of 14.82 g L<sup>-1</sup> cellobiose, 10.83 g L<sup>-1</sup> glucose, 6.36 g L<sup>-1</sup> xylose, 3.61 g L<sup>-1</sup> arabinose, 2.47 g L<sup>-1</sup> formic acid, 3.75 g L<sup>-1</sup> acetic acid, and 1.04 g L<sup>-1</sup> 5-HMF.

\* Corresponding authors.

E-mail addresses: [sganzerla.william@gmail.com](mailto:sganzerla.william@gmail.com) (W.G. Sganzerla), [taniafc@unicamp.br](mailto:taniafc@unicamp.br) (T. Forster-Carneiro).

<sup>1</sup> These authors contributed equally.

<https://doi.org/10.1016/j.supflu.2023.106004>

Received 12 January 2023; Received in revised form 29 May 2023; Accepted 2 June 2023

Available online 5 June 2023

0896-8446/© 2023 Elsevier B.V. All rights reserved.

## 1. Introduction

Lignocellulosic biomass consists of cellulose, hemicellulose, and lignin as major compounds. The diversity in the composition of biomass is responsible for the complexity of the processes used for pretreatment. Currently, biomass has been widely studied as a suitable feedstock to produce biofuels and biobased products, replacing fossil resources with a reduction in greenhouse gas (GHG) emissions [1,2]. Lignocellulosic biomass has been applied as feedstock to produce fuel, chemical products, proteins, amino acids, oligosaccharides, and phenolic compounds [3]. Nonetheless, ethanol and butanol are the typical products of interest in the biochemical route of biomass valorization [4]. An increase of up to nearly 400 % of the total biomass demand was projected for 2050 compared to 2011, resulting in a demand of up to 13.4 billion tons per year [5]. The abundance of lignocellulosic by-products from the agriculture and forest sectors appears to be a promising low-cost feedstock, such as corn fiber, wheat straw, brewer's spent grains (BSG), rice straw, and many others that can be used to obtain fermentable sugars at a relatively low cost [3].

BSG is produced in large amounts in the beer industry, accounting for 20 kg BSG for every 100 L beer processed [6]. The incorrect destination of BSG represents an issue in terms of environmental impact, however, BSG is a feedstock with a low financial aggregated value [7]. Cellulose (18 %), hemicellulose (35 %), and proteins (20 %) represent the major composition of BSG [6]. The management of BSG is a challenge for the beer industry, and novel alternatives based on sustainable processes should be investigated [8].

In a biorefinery concept, biomass conversion must first have a pretreatment to the hydrolysis of cellulose, hemicellulose, and lignin to produce a hydrolysate rich in sugar for its intended applications. Although the purpose is to maximize the recovery of fermentable sugars, pretreatment can produce several bioproducts, such as furfural, phenolic compounds, hydrolyzed fibers, and 5-HMF [9].

The use of sustainable biomass pretreatment should be explored to promote the sustainability and circular bioeconomy of the agri-food sector. SWH has been considered a sustainable pretreatment for the valorization of lignocellulosic biomass [9]. In the case of SWH, the temperature and pressure conditions of the water should be higher than its boiling point (100 °C, 1 MPa) and lower than its critical point (374 °C, 22 MPa) [10]. The dielectric constant of water in the subcritical state is close enough to several organic solvents, allowing hydrolysis reactions [11]. Although this pretreatment technique has high implementation and operational costs due to the requirement of high temperature and pressure, it is considered feasible and sustainable for the management of biomass by-products [9]. Previous studies described the optimal SWH pretreatment conditions to produce sugars and amino acids from BSG [12–14].

However, during the SWH of lignocellulosic materials, inhibitory compounds, such as furfural and 5-HMF, are formed, which are not suitable for biotechnological processes [15]. The inhibitors compounds have direct interference in the microbial growth and synergistic effects with other inhibitors in the interference of the fermentative process [16], causing damage to the cell wall, inhibiting microbial growth, reducing enzymatic activity, and consequently decreasing the fermentation yield [17,18]. At a high concentration, the inhibitors compounds can lead to deterioration or even cease activity in anaerobic reactors [19]. Therefore, the removal of inhibitors compounds generated during SWH should be investigated before the application of the hydrolysate in the fermentative process. Furfural can be easily removed by evaporation, however, the removal of 5-HMF should be better investigated. In addition, the isolation and purification of 5-HMF can be used as essential platform chemistry. The "Top 10 + 4" list by the U.S. Department of Energy contains 5-HMF as one of the most value-added chemicals [20].

Several methods have been reported in the literature for the removal of 5-HMF. Examples include adsorption, which is based on the adsorption of the 5-HMF into a solid material [21]. Biodegradation involves the

use of microorganisms capable of degrading 5-HMF into less harmful species [22], but it typically requires a lengthy process and is susceptible to complex and expensive operational parameters. Similarly, chemical degradation is possible but requires careful consideration of the formation of toxic by-products [23]. Membrane separation can be used based on size or molecular charge [24]; however, due to the heterogeneous nature of lignocellulosic biomass hydrolysates, it can be a challenge. Finally, liquid-liquid extraction is based on the greater affinity of the 5-HMF molecule to the solvent used, allowing for its separation from the hydrolysate. The choice of method depends on various factors, such as the source and concentration of 5-HMF, the desired product quality, and the economic and environmental feasibility of the method. In the case of liquid-liquid extraction, the parameters that affect the process are pH, temperature of separation, and the amount of solvent used in the process. These operational parameters should be better investigated to verify the effectiveness of liquid-liquid extraction to the detoxification and removal of 5-HMF.

Therefore, this study investigated the removal of 5-HMF from hydrolysate obtained by SWH of BSG. For this, liquid-liquid extraction was optimized at different temperatures, pH, and hydrolysate/ethyl acetate ratios. This study contributes to determining the appropriate conditions for the removal of 5-HMF from BSG hydrolysates, and the technique described can be applied to produce a purified hydrolysate for fermentative processes.

## 2. Materials and methods

### 2.1. Raw material

BSG was supplied by Ambev Brewery (Jaguariúna, SP, Brazil). The raw material was dried in an air convection oven (45 °C, 24 h) until reaching a moisture of 9 % (w/w). The size reduction was carried out in a multiprocessor until it reached an average particle size of 0.41 mm. The BSG used in this study presents 35.79 % hemicellulose, 17.90 % cellulose, and 17.87 % lignin [25].

### 2.2. Subcritical water hydrolysis

The SWH of BSG was conducted based on the process described in Fig. 1 (patent pending BR1020150314019). The system was composed of a high-pressure liquid pump (double piston pump, Model 36 preparation pump, Apple Valley, MN, USA) to pressurize and feed water to the subcritical reactor. The hydrolysis reactor consisted of 316-stainless steel tubes with an internal volume of 110 mL. A thermal jacket rated to deliver 1500 W was used to heat the reactor, insulated by a ceramic fiber jacket (RSA Equipment and Instrumentation, Campinas, SP, Brazil). The temperature was controlled using two thermocouples (type K) located at the entrance and outlet of the reactor. The product exiting the hydrolysis reactor was cooled in a serpentine coupled to a thermostatic bath (Marconi Equipment, model MA184, Piracicaba, SP, Brazil). The system's pressure is controlled by a micrometer valve (Parker Autoclave Engineers, model 10VRMM2812, Erie, PA, USA) located after the liquid exchanger. The pressure in the system was measured by pressure gauges (0–50 MPa) with an accuracy of up to 0.1 % (WIKA company, Klingenberg am Main, Bavaria, Germany).

The operational conditions used in the flow-through subcritical process were selected based on previous studies [12–14]. In each experiment, 10 g of BSG (dry basis) was loaded in the reactor, which was operated semicontinuous. The reactor was filled with water from the pump to reach pressures of 15 MPa and 180 °C in all experiments. The hydrolysis was performed with a water flow of 5 mL min<sup>-1</sup> and a solvent-to-feed ratio of 22.5 g water g<sup>-1</sup> feed. The hydrolysate was collected every 5 min for 45 min to determine the hydrolysis kinetics. In each hydrolysis, 225 mL of hydrolysate was obtained. In total, five hydrolysis were conducted to obtain a suitable volume of hydrolysate (approximately 1 L) for the experiment.

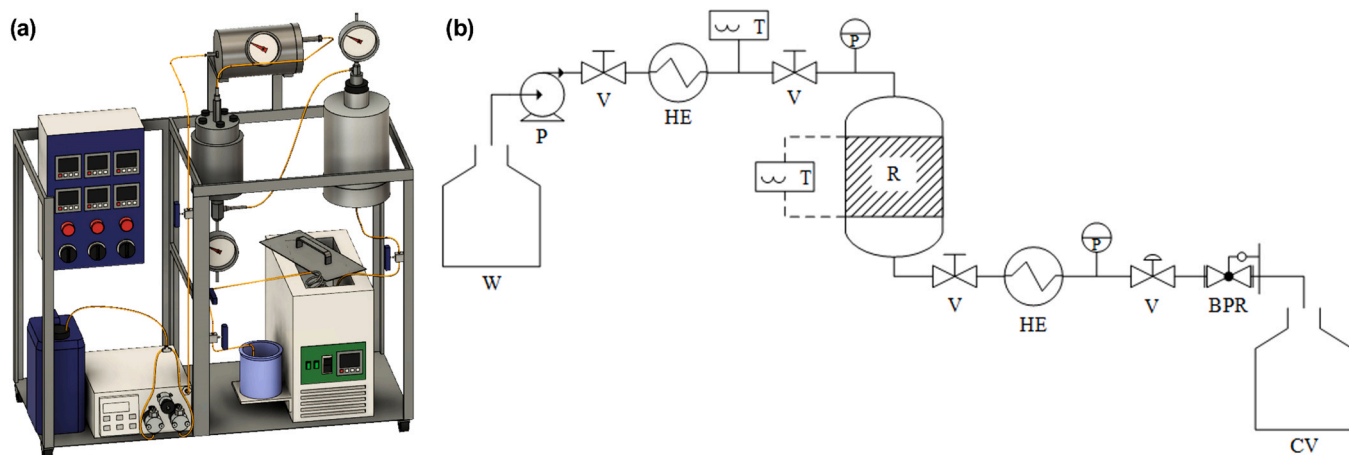


Fig. 1. Schematic diagram of the experimental apparatus for the semi-continuous SWH process. Label: W, water tank; P, high-pressure pump; V, block valves; P, manometer; T, thermocouples; R, hydrothermal reactor; HE, heat exchanger; MV, micrometric valve; CV, collecting vessel.

For the concentration of the hydrolysate previously obtained by SWH, 750 mL of the raw hydrolysate was concentrated under rotary evaporation (120 mbar, 50 °C, 10 rpm). The final volume of concentrated hydrolysate was 150 mL, while the volume of evaporated water was 600 mL. This step was necessary to increase the concentration of sugars in the hydrolysate. Based on the mass balance calculation, the raw hydrolysate was concentrated approximately 10-fold. The concentrated hydrolysate was used in the liquid-liquid extraction to remove 5-HMF.

### 2.3. Liquid-liquid extraction of 5-HMF from the concentrated hydrolysate

A selective method was applied to remove 5-HMF from the hydrolysate. The concentrated hydrolysate was subjected to liquid-liquid extraction using ethyl acetate to remove 5-HMF, already reported as an affinity solvent with the inhibitor [26–28]. The concentrated hydrolysate was mixed with ethyl acetate under different operating conditions and placed under stirring in an orbital shaker (Tecnal, Piracicaba, SP, Brazil) at 60 rpm for 40 min. Liquid-liquid extraction was performed using the concentrated hydrolysate at different pH (2.5, 4.5, and 6.5), temperatures (T) (25, 35, and 45 °C), and volumetric ratios of hydrolysate/ethyl acetate (H) (1:2, 1:1, and 2:1 v/v), according to the Box–Behnken design (Tables 1 and 2). After the liquid-liquid extraction the mixture was centrifuged (5000 rpm, 15 min, 20 °C) for phase separation. The aqueous phase (hydrolysate) was collected for analysis.

### 2.4. Analytical methods

#### 2.4.1. Sugars, organic acids, and inhibitors

Sugars, organic acids, furfural, and 5-HMF were analyzed by high-performance liquid chromatography (HPLC) with a refractive index detector (RID). Separation was performed using a Rezex™ column (Phenomenex, model ROA-Organic Acid H+ (8 %), 8 μm, 300 × 7.8 mm, Torrance, CA, USA), adopting an isocratic flow of

Table 1

Box–Behnken design optimization for the removal of 5-HMF from BSG hydrolysate obtained by SWH.

Variables	Code	Level		
		–1	0	1
pH	X <sub>1</sub>	2.5	4.5	6.5
T (°C)	X <sub>2</sub>	25	35	45
H (v/v)	X <sub>3</sub>	1:2	1:1	2:1

Label: T, temperature; H, the volumetric ratio between hydrolysate and ethyl acetate.

Table 2

Coded and uncoded independent variables for the Box–Behnken design to remove 5-HMF from BSG hydrolysate obtained by SWH.

Run	Coded variables			Uncoded variables			5-HMF removal (g L <sup>–1</sup> )	
	X <sub>1</sub>	X <sub>2</sub>	X <sub>3</sub>	pH	T (°C)	H (v/v)	Experimental	Predicted
1	–1	–1	0	2.5	25	1:1	1.71 ± 0.03	1.70
2	–1	1	0	2.5	45	1:1	1.59 ± 0.06	1.63
3	1	–1	0	6.5	25	1:1	1.67 ± 0.08	1.63
4	1	1	0	6.5	45	1:1	1.66 ± 0.07	1.66
5	–1	0	–1	2.5	35	1:2	1.16 ± 0.05	1.13
6	–1	0	1	2.5	35	2:1	2.29 ± 0.14	2.28
7	1	0	–1	6.5	35	1:2	1.04 ± 0.09	1.05
8	1	0	1	6.5	35	2:1	2.35 ± 0.12	2.37
9	0	–1	–1	4.5	25	1:2	1.35 ± 0.05	1.38
10	0	–1	1	4.5	25	2:1	2.42 ± 0.16	2.42
11	0	1	–1	4.5	45	1:2	1.25 ± 0.12	1.23
12	0	1	1	4.5	45	2:1	2.68 ± 0.14	2.66
13	0	0	0	4.5	35	1:1	1.75 ± 0.18	1.82
14	0	0	0	4.5	35	1:1	1.80 ± 0.15	1.82
15	0	0	0	4.5	35	1:1	1.92 ± 0.16	1.82

0.6 mL min<sup>–1</sup> of H<sub>2</sub>SO<sub>4</sub> (0.005 mol L<sup>–1</sup>) at 60 °C. The RID was maintained at 40 °C. For the analysis, the hydrolysates (raw, concentrated, and after liquid-liquid extraction) were centrifuged (10,000 rpm) for 15 min and filtered (cellulose acetate 0.22 μm). The hydrolysates were diluted 1:50 (v/v). Then, 20 μL of diluted hydrolysate was injected, and the run was established for 60 min. The concentrations of cellobiose, glucose, xylose, fructose, arabinose, formic acid, acetic acid, furfural, and 5-HMF were calculated from the calibration curves of each standard. The analysis was conducted in triplicate, and the results were expressed as g L<sup>–1</sup> hydrolysate.

#### 2.4.2. Phenolic compounds

Total phenolic compounds (TPC) were quantified using the Folin-Ciocalteu method [29]. The reaction was composed of 104 μL hydrolysate and diluted in 1667 μL of deionized water. The solution was reacted with 104 μL of Folin-Ciocalteu (0.25 N) reagent was added to the reaction, followed by incubation for 3 min in a dark environment. Next, 208 μL of sodium carbonate (1 mol L<sup>–1</sup>) was added to the reaction. After 2 h, the absorbance was measured in a spectrophotometer (Hach, model DR 4000 U, São Paulo, SP, Brazil) at 725 nm. The analysis was conducted in triplicate, and the results were expressed as g of gallic acid equivalent (GAE) L<sup>–1</sup> hydrolysate (g GAE L<sup>–1</sup>).

#### 2.4.3. Removal of 5-HMF

The removal of 5-HMF was calculated according to Eq. 1.

$$\text{Removal of 5-HMF (\%)} = \frac{\text{Initial}_{5\text{-HMF}} - \text{Final}_{5\text{-HMF}}}{\text{Initial}_{5\text{-HMF}}} \times 100 \quad (1)$$

where  $\text{Initial}_{5\text{-HMF}}$  is the concentration of 5-HMF in the concentrated hydrolysate and  $\text{Final}_{5\text{-HMF}}$  is the concentration of 5-HMF in the concentrated hydrolysate after liquid–liquid extraction.

### 2.5. Statistical modeling and optimization

The results obtained were submitted to analysis of variance (ANOVA) to assess the statistically significant factors and interaction effects between variables. The significant differences were determined by Tukey's test ( $p \leq 0.05$ ). The experimental results of 5-HMF removal were analyzed by response surface methodology (RSM) described by second-order equations (Eq. 2). The regression coefficients were determined for the response variables studied by the RSM. The significance test of regression coefficients was also confirmed by ANOVA ( $p \leq 0.05$ ). In addition, the response variables were optimized using the Simplex method.

$$Y_1 = \beta_0 + \sum_{i=1}^3 \beta_i X_i + \sum_{i=1}^3 \beta_{ii} X_i^2 + \sum_{i=1}^3 \sum_{j>i}^3 \beta_{ij} X_i X_j \quad (2)$$

where  $Y_1$  is the studied response variable;  $\beta_0$  is a constant;  $\beta_i$  are coefficients related to linear effects;  $\beta_{ii}$  are coefficients associated with quadratic effects;  $\beta_{ij}$  are coefficients for second-order cross terms;  $X_i$  is the variable  $i$  in the design; and  $X_j$  is the variable  $j$  in the design.

All statistical analyses were conducted in Statistica® software (version 10.0, StatSoft Inc., Tulsa, OK, USA).

## 3. Results and discussion

### 3.1. Kinetics of SWH

The kinetics of SWH (non-accumulated and accumulated) are presented in Fig. 2. The accumulated composition of the hydrolysate at the end of the process was cellobiose ( $1.43 \pm 0.11 \text{ g L}^{-1}$ ) as the major sugar, followed by glucose ( $1.06 \pm 0.12 \text{ g L}^{-1}$ ), xylose ( $0.53 \pm 0.08 \text{ g L}^{-1}$ ) and arabinose ( $0.28 \pm 0.04 \text{ g L}^{-1}$ ). The high cellobiose concentration indicates the efficiency in the hydrolysis of cellulose and hemicellulose of BSG [30], the major polysaccharides of BSG [31]. Cellobiose had maximum recovery in 5 min of hydrolysis. The other sugars were produced between 5 and 10 min, followed by a marked reduction at 30 min. In the accumulated profile of the sugars, a plateau in the kinetics was

observed. Similar behavior was observed by Georgalis et al. [32], who indicated the maximum content of sugars at 15 min of SWH.

Acetic acid was formed by the degradation reactions of mono-saccharides [33], which explains its continuous formation until the final hydrolysis process. In contrast, formic acid is possible formed by the degradation of furfural and 5-HMF [34], with a more accentuated formation from 10 min. At the end of the process, the formation of acetic acid ( $0.57 \pm 0.05 \text{ g L}^{-1}$ ) was higher than that of formic acid ( $0.37 \pm 0.01 \text{ g L}^{-1}$ ).

The presence of inhibitors increased with the hydrolysis time. These compounds are formed through more aggressive treatments, either by temperature or by longer hydrolysis time, promoting the breaking of the sugars in furfural, 5-HMF, and organic acids [35]. Furfural is produced by the breakdown of pentoses (five-carbon sugars), which results from the hydrolysis of hemicellulose from biomass. In contrast, 5-HMF is produced by the breakdown of hexoses (six-carbon sugars), which results from the hydrolysis of cellulose [36,37]. A hydrolysate with a high content of inhibitors is not desirable for biotechnological processes. 5-HMF had maximum formation at 15 min, followed by a decrease until the end of the process. This profile reflects that during SWH, the sugars are released followed by a subsequent conversion into inhibitors [38].

### 3.2. Composition of raw and concentrated hydrolysate

The raw and concentrated hydrolysate was quantified in mono-saccharides, organic acids, inhibitors, and phenolic compounds (Table 3). BSG presents 35.79 % hemicellulose, 17.90 % cellulose, and 17.87 % lignin [25]. The high composition of hemicellulose represents both a difficulty for biotechnological processes due to the complexity of

**Table 3**

Composition of raw and concentrated hydrolysate obtained by SWH.

Parameters	Raw hydrolysate	Concentrated hydrolysate	Unit
Cellobiose	$1.43 \pm 0.11$	$14.96 \pm 0.14$	$\text{g L}^{-1}$
Glucose	$1.06 \pm 0.12$	$10.91 \pm 0.13$	$\text{g L}^{-1}$
Xylose	$0.53 \pm 0.08$	$6.15 \pm 0.15$	$\text{g L}^{-1}$
Arabinose	$0.28 \pm 0.04$	$3.58 \pm 0.18$	$\text{g L}^{-1}$
Formic acid	$0.37 \pm 0.01$	$3.01 \pm 0.16$	$\text{g L}^{-1}$
Acetic acid	$0.57 \pm 0.05$	$5.56 \pm 0.14$	$\text{g L}^{-1}$
5-HMF	$0.48 \pm 0.02$	$3.98 \pm 0.13$	$\text{g L}^{-1}$
Furfural	$0.47 \pm 0.02$	n.d.	$\text{g L}^{-1}$
Phenolics	$1.26 \pm 0.13$	$10.57 \pm 0.44$	$\text{g L}^{-1}$

Label: n.d., not detected.

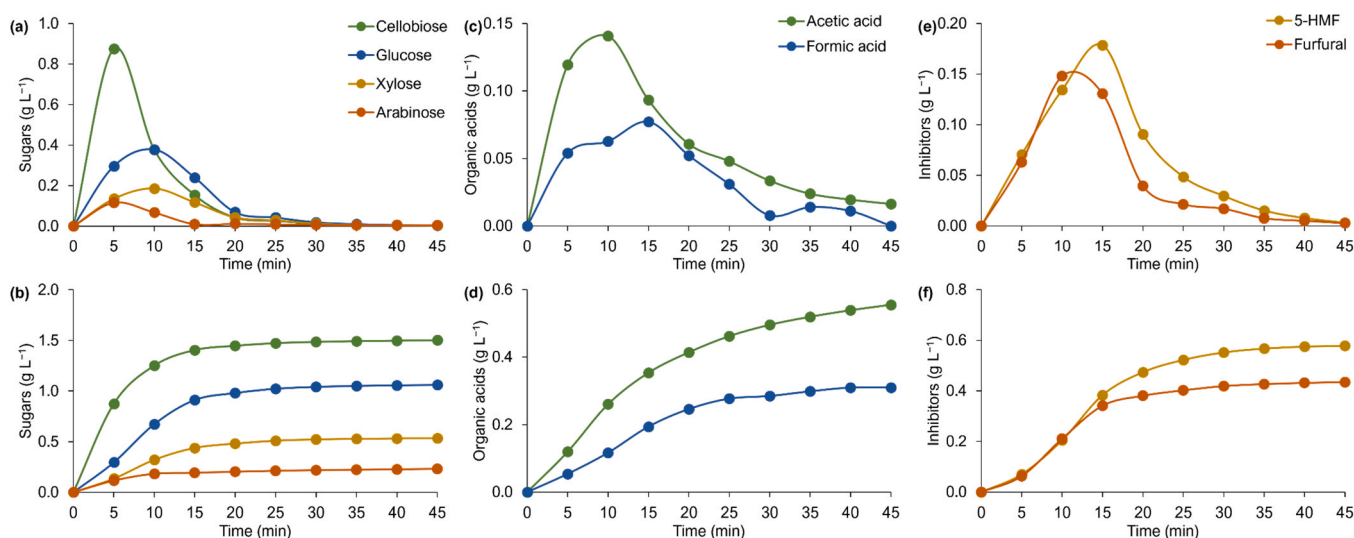


**Fig. 2.** Profile of sugars, organic acids, and inhibitors during the SWH of BSG. (a) sugars non-accumulated; (b) accumulated sugars; (c) organic acids non-accumulated; (d) accumulated organic acids; (e) inhibitors non-accumulated; and (f) accumulated inhibitors.

the sugar to be used by the enzymatic system of microorganisms [30], as well as advantages when using SWH, as it is easily converted into free sugars, such as xylose and arabinose [39]. The low concentrations of xylose ( $0.53 \pm 0.08 \text{ g L}^{-1}$ ) and arabinose ( $0.28 \pm 0.04 \text{ g L}^{-1}$ ) obtained in the raw hydrolysate may be associated with its rapid conversion of inhibitory compounds and organic acids. The hydrolysis of cellulose results in the production of glucose and cellobiose [40]. In the raw hydrolysate, cellobiose ( $1.43 \pm 0.11 \text{ g L}^{-1}$ ) and glucose ( $1.06 \pm 0.12 \text{ g L}^{-1}$ ) were obtained. According to Zeng et al. [30], a high concentration of cellobiose was obtained from the hydrolysis of BSG. The differences in the profile of sugars obtained are justified due to the influence of the barley species, harvest season, weather conditions, and processing conditions in the brewery, among other factors [41]. However, the composition of the raw hydrolysate corroborates previous studies of the SWH of BSG [12,14].

The concentrated hydrolysate presented  $35.6 \text{ g sugars L}^{-1}$ , a rich composition suitable for several biotechnological processes, such as the production of cellobionic acid by *Pseudomonas taetrolens* [42] and D-lactic acid from *Escherichia coli* [43], due to the higher concentration of cellobiose in the hydrolysate. Additionally, a medium with a high concentration of cellobiose was recently discovered to inhibit the conversion of deoxynivalenol-3-glucoside into its toxic precursor, deoxynivalenol, thus preventing damage to the human body [44]. However,  $3.98 \text{ g L}^{-1}$  5-HMF represents a barrier to the fermentative process [45]. While SWH pretreatment is an effective process to the hydrolysis of lignocellulosic biomass, one of its significant drawbacks is that it produces 5-HMF and, if not removed, could hinder microbial growth and inhibition during fermentation [45]. Thus, the removal of 5-HMF from the hydrolysate is ideal for promoting a more efficient fermentation process.

### 3.3. Hydrolysate composition after liquid–liquid extraction

The composition of the hydrolysates after liquid–liquid extraction is presented in Table 4. Overall, all treatments reduced 5-HMF, with a maximum of  $2.68 \text{ g L}^{-1}$  and a minimum of  $1.04 \text{ g L}^{-1}$ . From the Box–Behnken design, the Treatment 7 stood out with the removal of 73.87 % of 5-HMF from the concentrated hydrolysate. However, the other constituents changed in composition, probably caused by partial transfer losses to the phase containing ethyl acetate. This solvent is a short-chain ester of ethanol with acetic acid that is non-toxic, biodegradable, and low-cost. Due to its moderate polarity, it is an ecologically correct solvent [46,47]. Ethyl acetate is generally recognized as safe (GRAS) and is currently used as a solvent in the decaffeination of coffee and tea [48]. Its structure has two oxygen molecules, allowing greater removal capacity due to an interaction by hydrogen bonding with the structure of 5-HMF [49]. However, due to this polarity characteristic, some of the other compounds in the hydrolysate have reduced affinity

with the organic reagent, which would justify the migration, even if minimal, to the organic phase of the system (hydrolysate (water): ethyl acetate). The treatment with the greatest reduction of 5-HMF, for example, had a loss of 5 % of sugars, which we can consider minimal compared to the gains in biotechnological efficiency of hydrolysate with a lower concentration of 5-HMF. In contrast, some treatments and compounds that concentrated after the treatment can be seen, which can be caused by partial loss of water from the aqueous phase (hydrolysate), promoting the concentration of the compounds, or even interference from the pH of the medium and at low temperature of some treatments promoting hydrolysis reactions in the medium.

### 3.4. Removal efficiency of 5-HMF

Treatment 7 had the highest removal of 5-HMF (73.87 %), followed by treatments 5 (70.96 %) and 11 (68.56 %) (Fig. 3). The highest removal efficiency was achieved with a hydrolysate/ethyl acetate ratio of 1:2 (v/v), indicating that the higher extraction solvent ratio promotes the highest removal. This behavior was justified in Section 3.5 of the statistical evaluation of the process. In general, the more significant presence of ethyl acetate promotes a greater driving force for the diffusion of 5-HMF to its phase [50], and performing the extraction of the hydrogenated molecule of 5-HMF, 2,5-bishydroxymethylfuran, with ethyl acetate managed to remove 80 %. Similarly, Lang et al. [51] recovered 83 % of 5-HMF in a 1:1 (v/v) extract-to-solvent ratio. The results corroborate those of this study, which ensures the applicability of ethyl acetate for the liquid–liquid extraction of 5-HMF. The treatment with the lowest removal was 12 (32.72 %), followed by treatments 10 (39.32 %), 8 (41.06 %), and 6 (42.68 %). Both have the lowest ethyl acetate concentration, where the opposite behavior can be observed. The lower driving force in the organic phase decelerated and reduced the diffusion of 5-HMF to its phase.

The results of the 5-HMF removal found in this study were superior to those found by Bhatia et al. [52]. The study employed algae biochar to perform the adsorption removal of furfural and 5-HMF, resulting in a maximum removal value of only 47.96 %. This is similar to the behavior observed in the study by Bhatia et al. [53], which used biomass-derived pine biochar to remove 40 % of the phenolic compounds (furfural and 5-HMF) present in the hydrolysate. These results demonstrate the potential use of liquid–liquid extraction with ethyl acetate for removing 5-HMF from biomass hydrolysates.

The 5-HMF removed from the hydrolysate has other interests and applications. 5-HMF can be a biobased building block for biofuels, lubricants, and polymers [49]. 5-HMF can be subjected to oxidation, hydrogenation, and condensation reactions to obtain different products [54], such as ethyl levulinate [55], 2,5-furandicarboxylic acid [56], and 2,5-dimethylfuran [57]. 2,5-Dimethylfuran, for example, provides a higher energy density than ethanol, making it a competitive fuel in the

**Table 4**  
Composition of BSG hydrolysate obtained by SWH after liquid–liquid extraction.

Run	Cellobiose	Glucose	Xylose	Arabinose	Formic acid	Acetic acid	5-HMF	Phenolics	Unit
1	13.74 ± 0.23	10.21 ± 0.13	6.03 ± 0.03	2.90 ± 0.02	1.11 ± 0.08	3.36 ± 0.05	1.71 ± 0.03	10.27 ± 0.23	g L <sup>-1</sup>
2	12.90 ± 0.52	9.54 ± 0.09	5.45 ± 0.06	3.29 ± 0.04	2.63 ± 0.09	3.22 ± 0.07	1.59 ± 0.06	9.67 ± 0.82	g L <sup>-1</sup>
3	14.05 ± 0.61	10.09 ± 0.12	6.08 ± 0.02	3.47 ± 0.01	2.48 ± 0.14	3.62 ± 0.04	1.67 ± 0.08	10.45 ± 0.50	g L <sup>-1</sup>
4	14.67 ± 0.15	10.65 ± 0.11	6.11 ± 0.08	2.84 ± 0.06	2.93 ± 0.12	3.89 ± 0.11	1.66 ± 0.07	11.08 ± 0.92	g L <sup>-1</sup>
5	15.81 ± 0.17	11.42 ± 0.14	6.40 ± 0.05	2.95 ± 0.08	1.32 ± 0.15	3.21 ± 0.09	1.16 ± 0.05	10.93 ± 0.24	g L <sup>-1</sup>
6	12.84 ± 0.27	9.35 ± 0.12	5.44 ± 0.02	3.20 ± 0.03	1.92 ± 0.12	3.21 ± 0.10	2.29 ± 0.14	10.60 ± 0.54	g L <sup>-1</sup>
7	14.82 ± 0.52	10.83 ± 0.15	6.36 ± 0.07	3.61 ± 0.04	2.47 ± 0.17	3.75 ± 0.07	1.04 ± 0.09	11.20 ± 0.20	g L <sup>-1</sup>
8	14.27 ± 0.32	10.20 ± 0.17	6.05 ± 0.04	3.56 ± 0.02	2.79 ± 0.04	3.74 ± 0.09	2.35 ± 0.12	10.27 ± 0.29	g L <sup>-1</sup>
9	18.05 ± 0.12	13.13 ± 0.23	6.88 ± 0.08	3.87 ± 0.04	2.65 ± 0.14	3.80 ± 0.12	1.35 ± 0.05	11.28 ± 0.56	g L <sup>-1</sup>
10	13.92 ± 0.17	10.09 ± 0.18	5.52 ± 0.04	3.48 ± 0.05	2.65 ± 0.13	3.59 ± 0.14	2.42 ± 0.16	10.49 ± 0.65	g L <sup>-1</sup>
11	17.33 ± 0.19	12.43 ± 0.12	7.09 ± 0.09	3.96 ± 0.06	2.55 ± 0.12	3.83 ± 0.10	1.25 ± 0.12	11.75 ± 0.64	g L <sup>-1</sup>
12	15.17 ± 0.18	10.99 ± 0.12	6.22 ± 0.02	3.57 ± 0.04	2.53 ± 0.16	3.71 ± 0.07	2.68 ± 0.14	11.86 ± 0.80	g L <sup>-1</sup>
13	14.93 ± 0.23	10.71 ± 0.14	6.29 ± 0.05	3.60 ± 0.07	2.53 ± 0.14	3.73 ± 0.04	1.75 ± 0.18	11.04 ± 0.09	g L <sup>-1</sup>
14	14.96 ± 0.21	10.52 ± 0.15	5.68 ± 0.06	2.87 ± 0.02	3.02 ± 0.14	3.75 ± 0.09	1.80 ± 0.15	10.73 ± 0.52	g L <sup>-1</sup>
15	15.93 ± 0.31	11.38 ± 0.18	6.27 ± 0.03	3.77 ± 0.03	2.80 ± 0.12	3.78 ± 0.07	1.92 ± 0.16	10.52 ± 0.83	g L <sup>-1</sup>

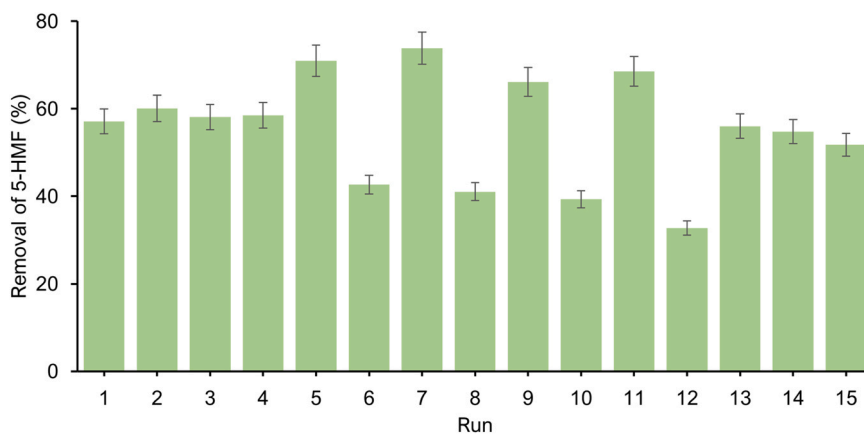


Fig. 3. Removal efficiency of 5-HMF from BSG hydrolysate after liquid-liquid extraction.

market, in addition to promising use in compression and spark ignition engines without the need to change the mechanical structure of the fuel engine [58].

### 3.5. Statistical modeling and optimization of the removal efficiency of 5-HMF

The effects of the different pH values, T, and H were investigated by a Box-Behnken design. A statistical model incorporating the second-order functions was evaluated for the response variable produced from SWH and analyzed by ANOVA. Fig. 4a shows the Pareto chart for 5-HMF removal. The factors H, pH<sup>2</sup>, H<sup>2</sup>, and T vs H had a significant statistical effect on the removal of 5-HMF from the samples at a significance level of 5 %. These results can also be observed in the ANOVA table (Table 5), and the residual error for the 5-HMF removal was  $\sqrt{2.75} = 1.66$ . The low residual error values indicated that the model could effectively predict the phenomenon involving the variables used in the experiment. This behavior can also be observed in Table 2 with the predictive values of 5-HMF that are close to the real values found.

Fig. 4b shows the plot between the predicted and observed values. It was possible to observe that the regression model adjusted the data efficiently, with a low dispersion of the data, where most of them are concentrated close to the predicted model curve, which indicates that the model adjusted the experimental data satisfactorily. Fig. 4c presents the histogram of raw residuals. From the histogram, it was possible to observe that the residuals are symmetrical around zero and that a normal distribution fits the data well. These observations regarding the residuals in the ANOVA satisfy the premise of parametric statistics and allow data analysis.

Three-dimensional response surfaces and level curves were generated for the statistically valid variable (Fig. 5). The 5-HMF removal was maximized at a lower H range in the dark burgundy region between

Table 5  
ANOVA results for the response surface statistical model for the removal of 5-HMF.

Parameters	SS	DF	MS	F	p	
pH (L)	0.06	1	0.06	0.02	0.89	n.s.
pH (Q)	86.90	1	86.90	31.66	0.00	*
T (L)	1.96	1	1.96	0.71	0.44	n.s.
T (Q)	1.35	1	1.35	0.49	0.52	n.s.
H (L)	1914.57	1	1914.57	697.45	0.00	*
H (Q)	37.05	1	37.05	13.50	0.01	*
pH (L) by T (L)	1.70	1	1.70	0.62	0.47	n.s.
pH (L) by H (L)	4.18	1	4.18	1.52	0.27	n.s.
T (L) by H (L)	24.98	1	24.98	9.10	0.03	*
Error	13.73	5	2.75			n.s.
Total SS	2068.00	14				n.s.

Label: SS, sum of squares; DF, degrees of freedom; MS, mean square; F, f value; p, p value; T, temperature; H, volumetric ratio of hydrolysate/ethyl acetate; L, linear effects; Q, quadratic effects; n.s., non-significant; \*, significant.

1:2.5 and 1:2 (v/v) (Fig. 5a), independent of the value for pH. The same behavior is observed in Fig. 5b with the T. According to Figs. 5c, 5-HMF removal was maximized at pH values of 2 and 7, independent of the value for T, which is the same behavior observed for the other two graphs. The equations for the interaction between T vs pH (Eq. 3), H vs pH (Eq. 4), H vs T (Eq. 5), and the determination coefficients for the adjusted regression model for the variables in the second-order functions were described.

$$Z = 64.62 - 8.33x_1 + 1.21x_1^2 + 0.60y_1 - 0.06y_1^2 - 0.03x_1y_1 \quad (R^2 = 0.993; R^2_{adj} = 0.981) \quad (3)$$

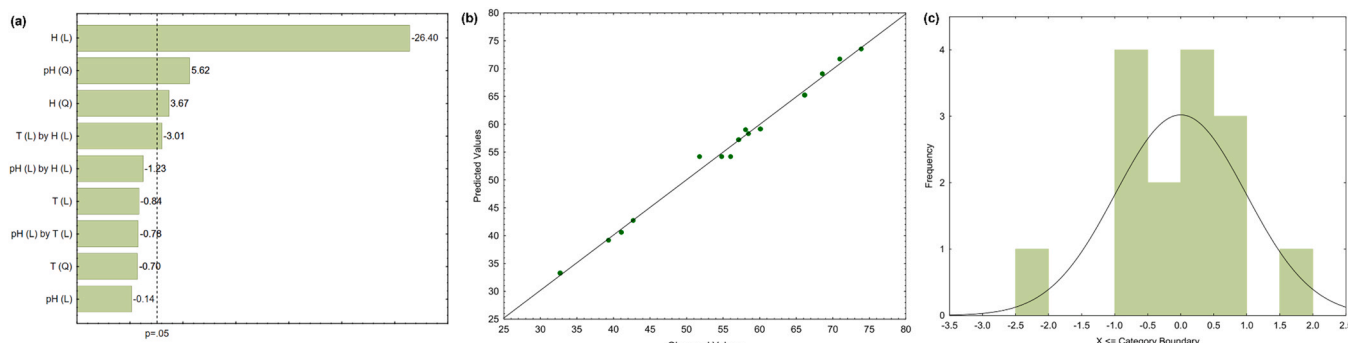


Fig. 4. (a) Pareto chart of standardized effects for the variable removal of 5-HMF; (b) Observed vs. predicted; and (c) histogram of raw residuals.

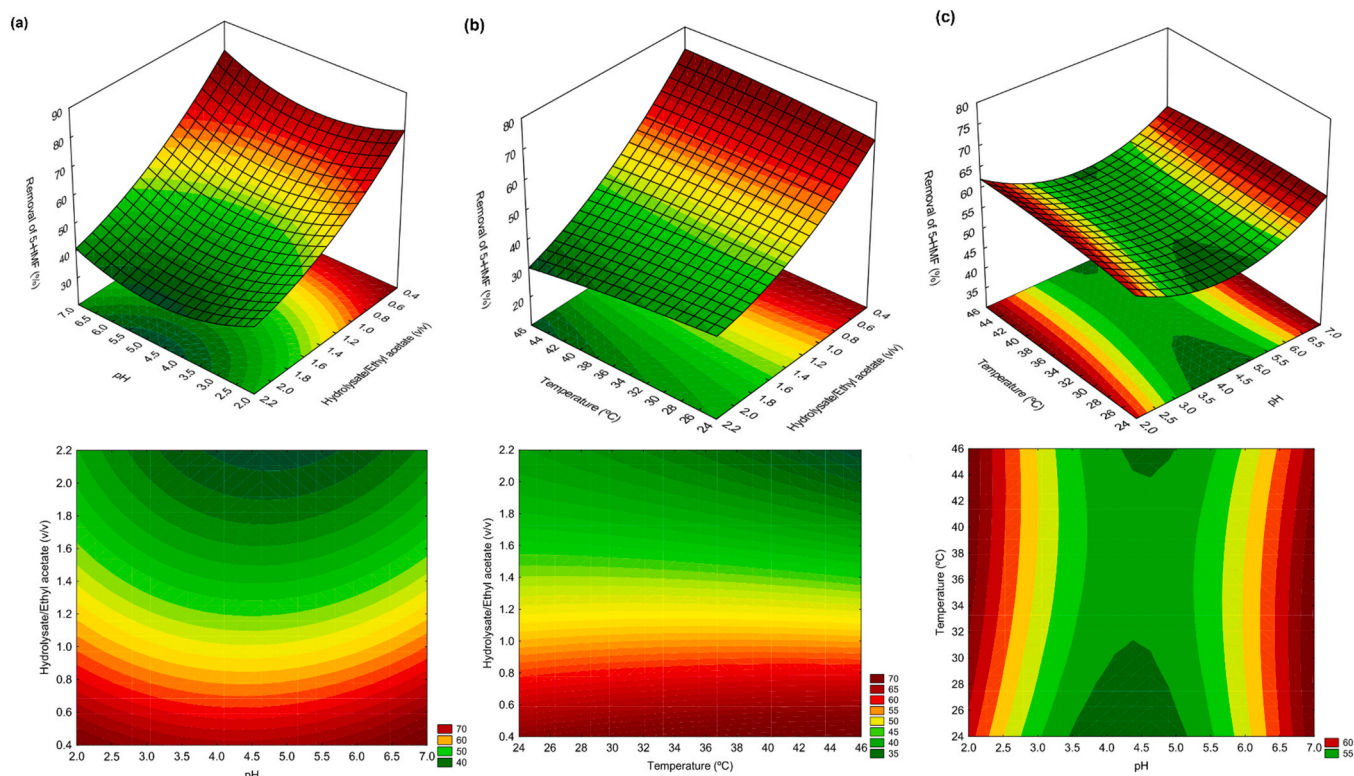


Fig. 5. Response surface plots for the removal efficiency of 5-HMF.

$$Z = 105.59 - 10.04x_2 + 1.21x_2^2 - 33.73y_2 + 6.49y_2^2 - 0.66x_2y_2 \quad (R^2 = 0.987; R^2_{\text{adj}} = 0.970) \quad (4)$$

$$Z = 64.76 + 0.785x_3 - 0.006x_3^2 - 25.50y_3 + 6.49y_3^2 - 0.32x_3y_3 \quad (R^2 = 0.973; R^2_{\text{adj}} = 0.962) \quad (5)$$

where  $Z$  represents the 5-HMF removal (%),  $x_1$  represents the pH,  $y_1$  represents the H (v/v),  $x_2$  represents the T (°C),  $y_2$  represents the H (v/v),  $x_3$  represents the pH, and  $y_3$  represents the T (°C).

It was observed that the determination coefficient ( $R^2$ ) was higher than 0.973, which indicates that the models competently fit the experimental data. To optimize the factorial design and maximize the value of the response variables, the models obtained were subjected to Simplex method analysis to determine the optimum value of the factors that generate the optimum removal of 5-HMF. The calculations were performed using the solver tool in Microsoft Office Excel®. The restrictions used in the software were the levels imposed by the experimental design: i)  $2.5 \leq \text{pH} \leq 6.5$ ; ii)  $25 \leq T \leq 45$  °C; and iii)  $1:2 \leq H \leq 2:1$ . The objective was the response variable itself. The optimization results for 5-HMF removal were pH = 6.5, T = 39 °C, H = 1:2, and 5-HMF removal = 72 %. These optimization conditions promoted a higher removal value for 5-HMF.

#### 4. Conclusion

This study evaluated the removal of 5-HMF by liquid–liquid extraction from BSG hydrolysate obtained by SWH. The optimal experimental conditions for liquid–liquid extraction were pH 6.5, 35 °C, and a volumetric ratio between hydrolysate and ethyl acetate of 1:2 (v/v). Under these conditions, up to 73.85 % of 5-HMF can be removed by the methodology described. The integration of SWH and liquid–liquid extraction can be an alternative to remove 5-HMF. Finally, this study advances the knowledge about the removal of undesirable compounds from BSG hydrolysates and contributes to the

application of this hydrolysate in fermentative processes. Future studies may explore the optimization of the 5-HMF removal process by reducing the amount of solvent utilized or by combining it with other removal methods. Furthermore, a comparative study can be conducted to assess the impact of the extracted 5-HMF on subsequent fermentation processes, thereby determining the optimal fermentative performance.

#### CRediT authorship contribution statement

**Tiago Linhares Cruz Tabosa Barroso:** Methodology, Investigation, Analysis, Validation, Writing – original draft. **William Gustavo Sganzerla:** Conceptualization, Methodology, Investigation, Validation, Writing – original draft, Writing – review & editing. **Luiz Eduardo Nochi Castro:** Investigation, Analysis, Writing – original draft. **Nícolas Luís Moreira Freiria:** Investigation, Analysis, Writing – original draft. **Gerardo Fernández Barbero:** Supervision, Writing – review & editing. **Miguel Palma Lovillo:** Supervision, Writing – review & editing. **Mauricio Ariel Rostagno:** Supervision, Resources, Writing – review & editing. **Tânia Forster-Carneiro:** Supervision, Resources, Project administration, Funding acquisition, Writing – review & editing.

#### Declaration of Competing Interest

The authors declare that they have no known competing financial interests or personal relationships that could have appeared to influence the work reported in this paper.

#### Data availability

Data will be made available on request.

#### Acknowledgements

This work was supported by the Brazilian Science and Research Foundation (CNPq, Brazil) (productivity grants 302451/2021-8);

Coordenação de Aperfeiçoamento de Pessoal de Nível Superior (CAPES, Brazil) (finance code 001); São Paulo Research Foundation (FAPESP, Brazil) (grant numbers 2018/14938-4 for T.F.C.; 2020/16248-5 for T.L.C.T.B.; 2019/26925-7 for W.G.S.; 2021/04096-9 for L.E.N.C.; 2018/14582-5 for M.A.R.).

## References

- [1] L.R. Lynd, G.T. Beckham, A.M. Guss, L.N. Jayakody, E.M. Karp, C. Maranas, R. L. McCormick, D. Amador-Noguez, Y.J. Bomble, B.H. Davison, C. Foster, M. E. Himmel, E.K. Holwerda, M.S. Laser, C.Y. Ng, D.G. Olson, Y. Román-Leshkov, C. T. Trinh, G.A. Tuskan, V. Upadhyay, D.R. Vardon, L. Wang, C.E. Wyman, Toward low-cost biological and hybrid biological/catalytic conversion of cellulosic biomass to fuels, *Energy Environ. Sci.* 15 (2022) 938–990, <https://doi.org/10.1039/D1EE02540F>.
- [2] S. Thanigaivel, S. Vickram, N. Dey, G. Gulothungan, R. Subbaiya, M. Govarthanan, N. Karmegam, W. Kim, The urge of algal biomass-based fuels for environmental sustainability against a steady tide of biofuel conflict analysis: is third-generation algal biorefinery a boon, *Fuel* 317 (2022), 123494, <https://doi.org/10.1016/j.fuel.2022.123494>.
- [3] A.A. Vertès, N. Qureshi, H.P. Blaschek, H. Yukawa (Eds.), *Biomass to Biofuels*, Wiley, 2010, <https://doi.org/10.1002/9780470750025>.
- [4] J. Habertzell, P. Hilgert, M. von Cossel, A critical review on lignocellulosic biomass yield modeling and the bioenergy potential from marginal land, *Agronomy* 11 (2021) 2397, <https://doi.org/10.3390/agronomy11122397>.
- [5] S. Piotrowski, M. Carus, R. Essel, Global bioeconomy in the conflict between biomass supply and demand, *Ind. Biotechnol.* 11 (2015) 308–315, <https://doi.org/10.1089/ind.2015.29021.stp>.
- [6] W.G. Sganzerla, L.C. Ampese, S.I. Mussatto, T. Forster-Carneiro, A bibliometric analysis on potential uses of brewer's spent grains in a biorefinery for the circular economy transition of the beer industry, *Biofuels Bioprod. Bioref.* 15 (2021) 1965–1988, <https://doi.org/10.1002/bbb.2290>.
- [7] F. Carvalheiro, L.C. Duarte, R. Medeiros, F.M. Gírio, Optimization of Brewery's spent grain dilute-acid hydrolysis for the production of pentose-rich culture media, *Appl. Biochem. Biotechnol.* 115 (2004) 1059–1072, <https://doi.org/10.1385/ABAB:115:1-3:1059>.
- [8] W.G. Sganzerla, L. Sillero, T. Forster-Carneiro, R. Solera, M. Perez, Determination of anaerobic co-fermentation of brewery wastewater and brewer's spent grains for bio-hydrogen production, *BioEnergy Res.* (2022), <https://doi.org/10.1007/s12155-022-10486-2>.
- [9] T.R. Sarker, F. Pattanaik, S. Nanda, A.K. Dalai, V. Meda, S. Naik, Hydrothermal pretreatment technologies for lignocellulosic biomass: a review of steam explosion and subcritical water hydrolysis, *Chemosphere* 284 (2021), 131372, <https://doi.org/10.1016/j.chemosphere.2021.131372>.
- [10] S.O. Essien, B. Young, S. Baroutian, Recent advances in subcritical water and supercritical carbon dioxide extraction of bioactive compounds from plant materials, *Trends Food Sci. Technol.* 97 (2020) 156–169, <https://doi.org/10.1016/j.tifs.2020.01.014>.
- [11] J.A. Okolie, S. Nanda, A.K. Dalai, F. Berruti, J.A. Kozinski, A review on subcritical and supercritical water gasification of biogenic, polymeric and petroleum wastes to hydrogen-rich synthesis gas, *Renew. Sustain. Energy Rev.* 119 (2020), 109546, <https://doi.org/10.1016/j.rser.2019.109546>.
- [12] W.G. Sganzerla, J. Viganó, L.E.N. Castro, F.W. Maciel-Silva, M.A. Rostagno, S. I. Mussatto, T. Forster-Carneiro, Recovery of sugars and amino acids from brewers' spent grains using subcritical water hydrolysis in a single and two sequential semi-continuous flow-through reactors, *Food Res. Int.* 157 (2022), 111470, <https://doi.org/10.1016/j.foodres.2022.111470>.
- [13] W.G. Sganzerla, G.L. Zabot, P.C. Torres-Mayanga, L.S. Buller, S.I. Mussatto, T. Forster-Carneiro, Techno-economic assessment of subcritical water hydrolysis process for sugars production from brewer's spent grains, *Ind. Crops Prod.* 171 (2021), 113836, <https://doi.org/10.1016/j.indcrop.2021.113836>.
- [14] P.C. Torres-Mayanga, S.P.H. Azambuja, M. Tyufekchiev, G.A. Tompssett, M. T. Timko, R. Goldbeck, M.A. Rostagno, T. Forster-Carneiro, Subcritical water hydrolysis of brewer's spent grains: selective production of hemicellulosic sugars (C-5 sugars), *J. Supercrit. Fluids* 145 (2019) 19–30, <https://doi.org/10.1016/j.supflu.2018.11.019>.
- [15] C.K. Yamakawa, F. Qin, S.I. Mussatto, Advances and opportunities in biomass conversion technologies and biorefineries for the development of a bio-based economy, *Biomass Bioenergy* 119 (2018) 54–60, <https://doi.org/10.1016/j.biombioe.2018.09.007>.
- [16] B.-B. Hu, J.-L. Wang, Y.-T. Wang, M.-J. Zhu, Specify the individual and synergistic effects of lignocellulose-derived inhibitors on biohydrogen production and inhibitory mechanism research, *Renew. Energy* 140 (2019) 397–406, <https://doi.org/10.1016/j.renene.2019.03.050>.
- [17] I. de, A. Bianchini, F.M. Joffre, S. de, S. Queiroz, T.M. Lacerda, M. das, G. de, A. Felipe, Relation of xylitol formation and lignocellulose degradation in yeast, *Appl. Microbiol. Biotechnol.* (2023), <https://doi.org/10.1007/s00253-023-12495-3>.
- [18] E. Gencturk, K.O. Ülgen, Understanding HMF inhibition on yeast growth coupled with ethanol production for the improvement of bio-based industrial processes, *Process Biochem.* 121 (2022) 425–438, <https://doi.org/10.1016/j.procbio.2022.07.015>.
- [19] Z. Tan, X. Li, C. Yang, H. Liu, J.J. Cheng, Inhibition and disinhibition of 5-hydroxymethylfurfural in anaerobic fermentation: a review, *Chem. Eng. J.* 424 (2021), 130560, <https://doi.org/10.1016/j.cej.2021.130560>.
- [20] J.J. Bozell, G.R. Petersen, Technology development for the production of biobased products from biorefinery carbohydrates—the US Department of Energy's "Top 10" revisited, *Green Chem.* 12 (2010) 539, <https://doi.org/10.1039/b922014c>.
- [21] S.K. Bhatia, R. Gurav, D.-H. Cho, B. Kim, H.J. Jung, S.H. Kim, T.-R. Choi, H.-J. Kim, Y.-H. Yang, Algal biochar mediated detoxification of plant biomass hydrolysate: mechanism study and valorization into polyhydroxyalkanoates, *Bioresour. Technol.* 370 (2023), 128571, <https://doi.org/10.1016/j.biortech.2022.128571>.
- [22] M.L. Becerra, L.M. Lizarazo, H.A. Rojas, G.A. Prieto, J.J. Martínez, Biotransformation of 5-hydroxymethylfurfural and furfural with bacteria of bacillus genus, *Biocatal. Agric. Biotechnol.* 39 (2022), 102281, <https://doi.org/10.1016/j.cbab.2022.102281>.
- [23] M.L. Krebs, A. Bodach, C. Wang, F. Schüth, Stabilization of alkaline 5-HMF electrolytes via Cannizzaro reaction for the electrochemical oxidation to FDCA, *Green Chem.* 25 (2023) 1797–1802, <https://doi.org/10.1039/D2GC04732B>.
- [24] A. Sarwono, Z. Man, A. Idris, A.S. Khan, N. Muhammad, C.D. Wilfred, Optimization of ionic liquid assisted sugar conversion and nanofiltration membrane separation for 5-hydroxymethylfurfural, *J. Ind. Eng. Chem.* 69 (2019) 171–178, <https://doi.org/10.1016/j.jiec.2018.09.020>.
- [25] W.G. Sganzerla, J. Viganó, L.E.N. Castro, F.W. Maciel-Silva, M.A. Rostagno, S. I. Mussatto, T. Forster-Carneiro, Recovery of sugars and amino acids from brewers' spent grains using subcritical water hydrolysis in a single and two sequential semi-continuous flow-through reactors, *Food Res. Int.* 157 (2022), 111470, <https://doi.org/10.1016/j.foodres.2022.111470>.
- [26] G.R. Gomes, J.C. Pastre, Microwave-assisted HMF production from water-soluble sugars using betaine-based natural deep eutectic solvents (NADES), *Sustain Energy Fuels* 4 (2020) 1891–1898, <https://doi.org/10.1039/C9SE01278H>.
- [27] G.A.D. Castro, S.A. Fernandes, R. de, C.S. de Sousa, M.M. Pereira, Green synthesis of 5-hydroxymethylfurfural and 5-acetoxymethylfurfural using a deep eutectic solvent in a biphasic system assisted by microwaves, *React. Chem. Eng.* (2023), <https://doi.org/10.1039/D2RE00399F>.
- [28] V.M. Nascimento, J.L. Ienczak, R. Boni, R. Maciel Filho, S.C. Rabelo, Mapping potential solvents for inhibitors removal from sugarcane bagasse hemicellulosic hydrolysate and its impact on fermentability, *Ind. Crops Prod.* 192 (2023), 116023, <https://doi.org/10.1016/j.indcrop.2022.116023>.
- [29] J.A. SINGLETON, V.L. ROSSI, Colorimetry of total phenolics with phosphomolybdic-phosphotungstic acid reagents, *Am. J. Enol. Vitic.* 16 (1965) 144–158.
- [30] J. Zeng, W. Huang, X. Tian, X. Hu, Z. Wu, Brewer's spent grain fermentation improves its soluble sugar and protein as well as enzymatic activities using *Bacillus velezensis*, *Process Biochem.* 111 (2021) 12–20, <https://doi.org/10.1016/j.procbio.2021.10.016>.
- [31] J. Steiner, S. Procopio, T. Becker, Brewer's spent grain: source of value-added polysaccharides for the food industry in reference to the health claims, *Eur. Food Res. Technol.* 241 (2015) 303–315, <https://doi.org/10.1007/s00217-015-2461-7>.
- [32] L. Georgalis, A. Psaroulaki, A. Aznar, P.S. Fernández, A. Garre, Different model hypotheses are needed to account for qualitative variability in the response of two strains of *Salmonella* spp. under dynamic conditions, *Food Res. Int.* 158 (2022), 111477, <https://doi.org/10.1016/j.foodres.2022.111477>.
- [33] H. Ishak, H. Yoshida, N.A. Muda, M.H.S. Ismail, S. Izhar, Rapid processing of abandoned oil palm trunks into sugars and organic acids by sub-critical water, *Processes* 7 (2019) 593, <https://doi.org/10.3390/pr7090593>.
- [34] T. Barroso, W. Sganzerla, R. Rosa, L. Castro, F. Maciel-Silva, M. Rostagno, T. Forster-Carneiro, Semi-continuous flow-through hydrothermal pretreatment for the recovery of bioproducts from jabuticaba (*Myrciaria cauliflora*) agro-industrial by-product, *Food Res. Int.* 158 (2022), 111547, <https://doi.org/10.1016/j.foodres.2022.111547>.
- [35] F.W. Maciel-Silva, S.I. Mussatto, T. Forster-Carneiro, Integration of subcritical water pretreatment and anaerobic digestion technologies for valorization of açai processing industries residues, *J. Clean. Prod.* 228 (2019) 1131–1142, <https://doi.org/10.1016/j.jclepro.2019.04.362>.
- [36] Ó. Benito-Román, P. Alonso-Riño, E. Díaz de Cerio, M.T. Sanz, S. Beltrán, Semi-continuous hydrolysis of onion skin wastes with subcritical water: pectin recovery and oligomers identification, *J. Environ. Chem. Eng.* 10 (2022), 107439, <https://doi.org/10.1016/j.jece.2022.107439>.
- [37] T.L.C.T. Barroso, R.G. da Rosa, W.G. Sganzerla, L.E.N. Castro, F.W. Maciel-Silva, M. A. Rostagno, T. Forster-Carneiro, Hydrothermal pretreatment based on semi-continuous flow-through sequential reactors for the recovery of bioproducts from jabuticaba (*Myrciaria cauliflora*) peel, *J. Supercrit. Fluids* 191 (2022), 105766, <https://doi.org/10.1016/j.supflu.2022.105766>.
- [38] J.A. Rojas-Chamorro, J.M. Romero-García, C. Cara, I. Romero, E. Castro, Improved ethanol production from the slurry of pretreated brewers' spent grain through different co-fermentation strategies, *Bioresour. Technol.* 296 (2020), 122367, <https://doi.org/10.1016/j.biortech.2019.122367>.
- [39] P.C. Torres-Mayanga, S.P.H. Azambuja, M. Tyufekchiev, G.A. Tompssett, M. T. Timko, R. Goldbeck, M.A. Rostagno, T. Forster-Carneiro, Subcritical water hydrolysis of brewer's spent grains: selective production of hemicellulosic sugars (C-5 sugars), *The J. Supercrit. Fluids* 145 (2019) 19–30, <https://doi.org/10.1016/j.supflu.2018.11.019>.
- [40] F. Gu, H. Liu, Hydroxyl radicals-mediated oxidative cleavage of the glycosidic bond in cellobiose by copper catalysts and its application to low-temperature depolymerization of cellulose, *Chin. J. Catal.* 41 (2020) 1073–1080, [https://doi.org/10.1016/S1872-2067\(20\)63569-0](https://doi.org/10.1016/S1872-2067(20)63569-0).

- [41] T. Amoriello, R. Ciccoritti, Sustainability: recovery and reuse of brewing-derived by-products, *Sustainability* 13 (2021) 2355, <https://doi.org/10.3390/su13042355>.
- [42] Y.-R. Oh, G.T. Eom, Efficient production of cellobionic acid from cellobiose by genetically modified *Pseudomonas taetrolens*, *Biochem. Eng. J.* 178 (2022), 108282, <https://doi.org/10.1016/j.bej.2021.108282>.
- [43] Y. Aso, M. Tsubaki, B.H. Dang Long, R. Murakami, K. Nagata, H. Okano, N. T. Phuong Dung, H. Ohara, Continuous production of d-lactic acid from cellobiose in cell recycle fermentation using  $\beta$ -glucosidase-displaying *Escherichia coli*, *J. Biosci. Bioeng.* 127 (2019) 441–446, <https://doi.org/10.1016/j.jbiosc.2018.09.011>.
- [44] K. Li, L. Wang, D. Yu, Z. Yan, N. Liu, A. Wu, Cellobiose inhibits the release of deoxynivalenol from transformed deoxynivalenol-3-glucoside from *Lactiplantibacillus plantarum*, *Food Chem. Mol. Sci.* 4 (2022), 100077, <https://doi.org/10.1016/j.fochms.2022.100077>.
- [45] T.R. Sarker, F. Pattnaik, S. Nanda, A.K. Dalai, V. Meda, S. Naik, Hydrothermal pretreatment technologies for lignocellulosic biomass: a review of steam explosion and subcritical water hydrolysis, *Chemosphere* 284 (2021), 131372, <https://doi.org/10.1016/j.chemosphere.2021.131372>.
- [46] A.Y. Adesina, I.B. Obot, S. Ahmad.A. Sorour, S.B. Mtongana, A.A. Mamilla, Almathami, Corrosion challenges and prevention in Ethyl Acetate (EA) production and related processes – an overview, *Eng. Fail. Anal.* 127 (2021), 105511, <https://doi.org/10.1016/j.engfailanal.2021.105511>.
- [47] S. Zhang, F. Guo, W. Yan, W. Dong, J. Zhou, W. Zhang, F. Xin, M. Jiang, Perspectives for the microbial production of ethyl acetate, *Appl. Microbiol. Biotechnol.* 104 (2020) 7239–7245, <https://doi.org/10.1007/s00253-020-10756-z>.
- [48] D.O.H.A.H. Services, Food and Drug Administration, in: Code of Federal Regulations, third ed., Silver Spring, 2022.
- [49] E.C. Sindermann, A. Holbach, A. de Haan, N. Kockmann, Single stage and countercurrent extraction of 5-hydroxymethylfurfural from aqueous phase systems, *Chem. Eng. J.* 283 (2016) 251–259, <https://doi.org/10.1016/j.cej.2015.07.029>.
- [50] T. Wang, J. Wei, H. Liu, Y. Feng, X. Tang, X. Zeng, Y. Sun, T. Lei, L. Lin, Synthesis of renewable monomer 2, 5-bishydroxymethylfuran from highly concentrated 5-hydroxymethylfurfural in deep eutectic solvents, *J. Ind. Eng. Chem.* 81 (2020) 93–98, <https://doi.org/10.1016/j.jiec.2019.08.057>.
- [51] J. Lang, J. Lu, P. Lan, N. Wang, H. Yang, H. Zhang, Preparation of 5-HMF in a DES/ethyl N-butylate two-phase system, *Catalysts* 10 (2020) 636, <https://doi.org/10.3390/catal10060636>.
- [52] S.K. Bhatia, R. Gurav, D.-H. Cho, B. Kim, H.J. Jung, S.H. Kim, T.-R. Choi, H.-J. Kim, Y.-H. Yang, Algal biochar mediated detoxification of plant biomass hydrolysate: mechanism study and valorization into polyhydroxyalkanoates, *Bioresour. Technol.* 370 (2023), 128571, <https://doi.org/10.1016/j.biortech.2022.128571>.
- [53] S.K. Bhatia, R. Gurav, B. Kim, S. Kim, D.-H. Cho, H. Jung, Y.-G. Kim, J.-S. Kim, Y.-H. Yang, Coproduction of exopolysaccharide and polyhydroxyalkanoates from *Sphingobium yanoikuyae* BBL01 using biochar pretreated plant biomass hydrolysate, *Bioresour. Technol.* 361 (2022), 127753, <https://doi.org/10.1016/j.biortech.2022.127753>.
- [54] Z. Tan, Y. Liu, H. Liu, C. Yang, Q. Niu, J.J. Cheng, Effects of 5-hydroxymethylfurfural on removal performance and microbial community structure of aerobic activated sludge treating digested swine wastewater, *J. Environ. Chem. Eng.* 9 (2021), 106104, <https://doi.org/10.1016/j.jece.2021.106104>.
- [55] C. P.A. S. Darbha, Catalytic conversion of HMF into ethyl levulinate – a biofuel over hierarchical zeolites, *Catal. Commun.* 140 (2020), 105998, <https://doi.org/10.1016/j.catcom.2020.105998>.
- [56] Y.-T. Liao, V.C. Nguyen, N. Ishiguro, A.P. Young, C.-K. Tsung, K.C.-W. Wu, Engineering a homogeneous alloy-oxide interface derived from metal-organic frameworks for selective oxidation of 5-hydroxymethylfurfural to 2,5-furandicarboxylic acid, *Appl. Catal. B Environ.* 270 (2020), 118805, <https://doi.org/10.1016/j.apcatb.2020.118805>.
- [57] W. Han, M. Tang, J. Li, X. Li, J. Wang, L. Zhou, Y. Yang, Y. Wang, H. Ge, Selective hydrogenolysis of 5-hydroxymethylfurfural to 2,5-dimethylfuran catalyzed by ordered mesoporous alumina supported nickel-molybdenum sulfide catalysts, *Appl. Catal. B Environ.* 268 (2020), 118748, <https://doi.org/10.1016/j.apcatb.2020.118748>.
- [58] H. Son Le, Z. Said, M. Tuan Pham, T. Hieu Le, I. Veza, V. Nhanh Nguyen, B. Deepanraj, L. Huong Nguyen, Production of HMF and DMF biofuel from carbohydrates through catalytic pathways as a sustainable strategy for the future energy sector, *Fuel* 324 (2022), 124474, <https://doi.org/10.1016/j.fuel.2022.124474>.